Mesh optimization for ground vehicle Aerodynamics

Ahmad, NE, Abo-Serie, E & Gaylard, A

Original citation:
Ahmad, NE, Abo-Serie, E & Gaylard, A 2010, 'Mesh optimization for ground vehicle Aerodynamics' *CFD Letters*, vol 2, no. 1, pp. 54-65

ISSN 2180-1363

Publisher: CFD Letters & ISSR Journals

CFD Letters www.cfdl.issres.net Vol. 2(1) – March 2010

Mesh Optimization for Ground Vehicle Aerodynamics

Nor Elyana Ahmad[1] and Essam Abo-Serie[1c] and Adrian Gaylard[2]
[1] *Mechanical and Automotive Engineering Department, Faculty of Engineering and Computing, Coventry University, UK*
[2] *Jaguar Land Rover, Aerodynamics.*

Received: 23/10/2009 – Revised 07/11/2010 – Accepted 15/02/2010

Abstract

A mesh optimization strategy for accurately estimating the drag of a ground vehicle is proposed based on examining the effect of different mesh parameters. The optimized mesh parameters were selected using a Design of Experiments (DoE) method enabling simulations to be carried out in a limited memory environment, and in a timely manner; without compromising the accuracy of results. The study was extended to take into account the effect of model size. A simplified car model at three scales has been investigated and compared with results from the MIRA model wind tunnel. Parameters that lead to drag values closer to experiment with less memory and computational time have been identified. Scaling the optimized mesh size with the length of car model was successfully used to predict the drag of the other car sizes with reasonable accuracy. This investigation was carried out using STAR-CCM+, a commercial CFD package; however the findings can be applied to any similar CFD code.

Keywords: Mesh optimization; Aerodynamics; Ground Vehicle CFD; Vehicle Drag

1. Introduction and Literature Review

One of the most important requirements before carrying out a CFD computation is mesh generation. In order to produce accurate results, it is essential to understand the influence of mesh size. Obtaining a completely mesh independent solution could be very expensive and time consuming, particularly if the mesh size is reduced erratically. To have a suitable mesh density for a specific problem with acceptable CPU time and numerical accuracy has remained a major theme in the CFD literature. The flow pattern around a vehicle is very complex and relatively large. To be able to resolve the wakes behind the vehicle, a fine mesh is required. However to reduce the computation time and memory, a strategy has to be established to refine the mesh only in particular areas within the flow domain.

The common practice in vehicle aerodynamics studies is to perform local refinement near the vehicle surface and in the areas of relatively high velocity gradients. Nevertheless a coarser mesh is kept at the far field fluid domain [1, 2, 3]. A mesh independency study is then carried out in order to

[c] Corresponding Author: E. Abo-Serie
Email: e.abo-serie@coventry.ac.uk Telephone: +44(0)2476887897 Fax: +02476888272

ensure that the solution is independent of the mesh size. This is usually achieved through a further reduction in mesh size until a small difference in the drag coefficient between two successive mesh refinements is reached. This process continues until the difference in the drag coefficient is below 0.003 [1] or less than 5% [2].

Most of the mesh optimization related research is concerned with adaptation and refinement of the mesh size during the solution process [4, 5]. Reconstruction of the grid for vehicle aerodynamics could be very time consuming as the flow domain is relatively large and not necessarily beneficial. Constructing a well distributed mesh from the beginning can eliminate the need to implement adaptive mesh techniques. All CFD software packages can automatically generate mesh based on pre-set values, however it is important to have appropriate initial setting values.

This study provides guidelines in generating mesh for solving aerodynamics flow over three sizes of fast back car models. It recommends initial values for different mesh parameters to reduce computation time and memory. The generated mesh could be used as an initial mesh if a solution adaptive meshing strategy is used. Parameters, named boundary specific surface size (in this case, the car surface), surface growth rate, mesh types, number of prism layers and prism layer thickness are studied.

2. Mesh Optimization Methodology

The strategy to reach the optimum mesh setting followed four stages:

- First stage – mesh base size selection
- Second stage – comparison between full and half car model
- Third stage – mesh parameters optimization using statistical analysis.
- Fourth stage – changes in mesh parameters as the car size becomes smaller.

The study was carried out on the MIRA Reference Car fast-back variant [6]. The first three stages were carried out using a 1:3 scale model; the fourth stage, used three scales: 1:3, 1:4 and 1:5.

The simulations were run using STAR-CCM+ version 4.04 and the computation was carried out on Intel Core 2 Duo 3GHz processors with 3GB RAM. The drag coefficient results obtained from the CFD for the three model sizes were validated with experimental results from the MIRA model wind tunnel as shown in Table 1 (below). The drag coefficient value increases as the model size enlarges as a result of blockage effects. Different studies have been conducted to correct for this effect experimentally [7] and using CFD [8]. Hence, there are two variables affecting the mesh optimization process here: model size and wind tunnel blockage.

TABLE 1: MIRA DRAG COEFFICIENTS MEASUREMENTS FOR FAST-BACK MODEL [6]

Model scale	Drag Coefficient
1:5	0.2653
1:4	0.2706
1:3	0.3208

3. CFD Model Setting

3.1. Model Installation in the MIRA Model Wind Tunnel

Figure 1 (below) shows the model position in MIRA model wind tunnel. In its pre-1996 configuration it was an open-return type, with a closed rectangular test section with

dimensions as shown in figure 1 [9]. The model was aligned at zero yaw in the wind tunnel [6].

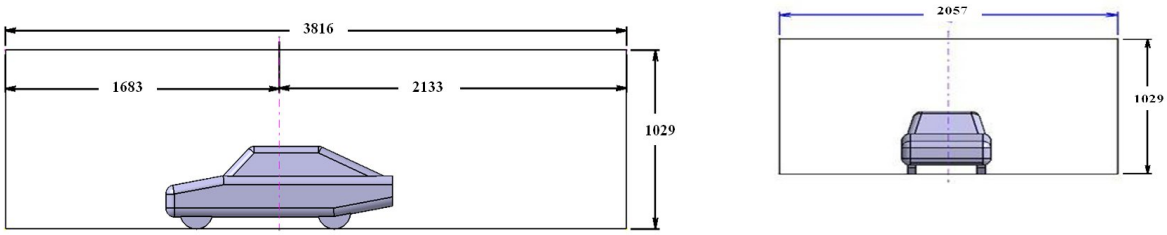

Figure 1. Model installation in the MIRA model wind tunnel

3.2. Boundary Conditions

The floor, walls and ceiling of the test section are treated as a non-slip wall imitating the wind tunnel conditions. The inlet condition is specified as a velocity inlet and the outlet condition is specified as a pressure outlet at atmospheric pressure. For all the three size models, the wind tunnel air speed was chosen to maintain Reynolds number at approximately 10^6. Accordingly, the air velocity used with each of the three model sizes was calculated, as shown in Table 2. This velocity was used in the wind tunnel as well as the inlet velocity for the CFD models.

TABLE 2: WIND TUNNEL AIR SPEED FOR EACH SCALE MODEL [7]

Model Scale	Model length (m)	Wind tunnel air speed (m/s)
1:3	1.388	11.3
1:4	1.041	15.0
1:5	0.833	18.8

According to previous studies [10, 11], the recommended domain size for automotive aerodynamics calculations provides clearances of between two and three car lengths upstream, five car lengths downstream, and twice the car height vertically. These values have *not* been followed in this investigation, as the aim is to provide a comparative study rather than absolute values. The dimensions as shown in figure 1 have been considered as the fluid flow domain. These might introduce some additional error but it is believed this will not affect the aim and the conclusions drawn from this study.

3.3. Problem Definitions and Assumptions

The fluid flow Reynolds-averaged Navier-Stokes RANS equations are solved assuming incompressible flow since the Mach number is below 0.3. To reduce the computation time, the energy equation can be excluded as there is no heat transfer or temperature change. Steady flow is also assumed since the aim is not to investigate the vortex fluctuations which are commonly formed in wake behind a car. The segregated flow algorithm is sufficient in this case, as it provides convergence for the range of vehicle speeds considered. The realizable K-Epsilon (k-ε) turbulence model is used in this study as it is commonly used in external vehicle aerodynamics studies [See 1, 12 and 13, for example]. The simple car model used in this study has fully closed surfaces with no internal flow.

4. Results and Discussion

In this project, the experimental drag coefficient values were assumed to be correct; although, it is known that the difference in drag coefficient values tested in different wind tunnels for the same car could be up to 5% [14].

4.1. First Stage – Mesh Base Size Selection

In the first stage, mesh base sizes of 50 mm and 100 mm, which are approximately 3.6% and 7.2% of car length, were compared. The mesh within the flow domain around the car was divided into four zones, named volumetric control regions, as shown in figure 2. The cells near the surface were set to be 25% of the mesh base size, increasing to 30% of the base mesh size in the first region. A polyhedral mesher was used for the core mesh and two prism layers of thickness 33.3% of the mesh base size. These prism layers were used in an attempt to provide an accurate estimation of the velocity near the wall, when using the wall function, by keeping the y-plus value within an acceptable range (20 to 200) [3].

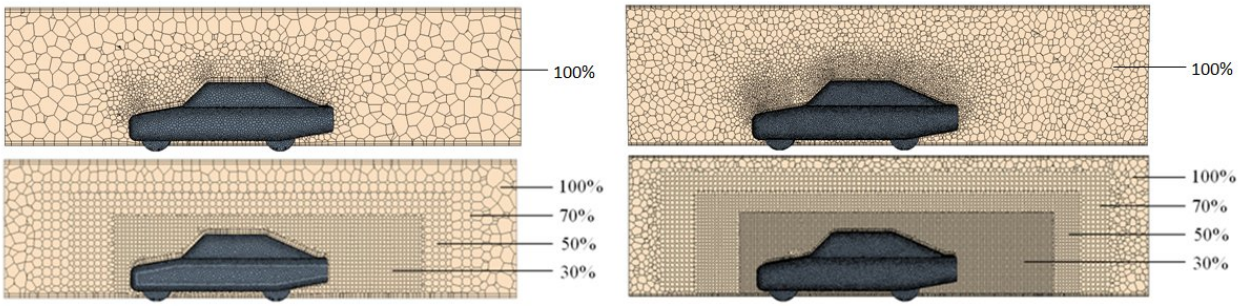

Figure 2. Mesh without volumetric control (top) and four zones of meshing with volumetric control (below). The mesh base size is 100mm (left) and 50mm (right); and the car surface mesh size is 25%. All dimensions are expressed as percentage of mesh base size.

Table 3 (below) lists the calculated drag coefficients for two mesh configurations; one for a four-zone mesh 'with volumetric control' and the other for 'without volumetric control', both cases were run at two base sizes 50 mm and 100mm.

TABLE 3: SIMULATION RESULTS COMPARING DIFFERENT MESH SIZES

Mesh base size (mm)	Drag Coefficient at 250 iterations			Simulation running time (min) at 250 iterations		
	No volumetric control	With volumetric control	Percentage difference*	No volumetric control	With volumetric control	Percentage difference*
100	0.367814	0.3487	5.5%	18	25	28%
50	0.337598	0.3345	0.9%	68	174	61%

* Percentage difference is calculated by adopting the 'with volumetric control' as the reference. (The measured drag coefficient for the 1:3 scale model is 0.3208.)

It is apparent from table 3 above that the finer the mesh, the closer the simulated drag coefficient is to the experimental value, and as expected, the more time is required to run the simulation. Comparing 100mm and 50mm mesh base sizes, the 50mm requires about 4

times more simulation run time without volumetric control and 7 times more with volumetric control. Generally, a finer mesh around the vehicle using control volume gives a more accurate drag coefficient result, but needs more computing time, compared to the case without volumetric control. The smaller cells around the model also provide better resolution of the wake region behind the car, as shown in figure 3 (below).

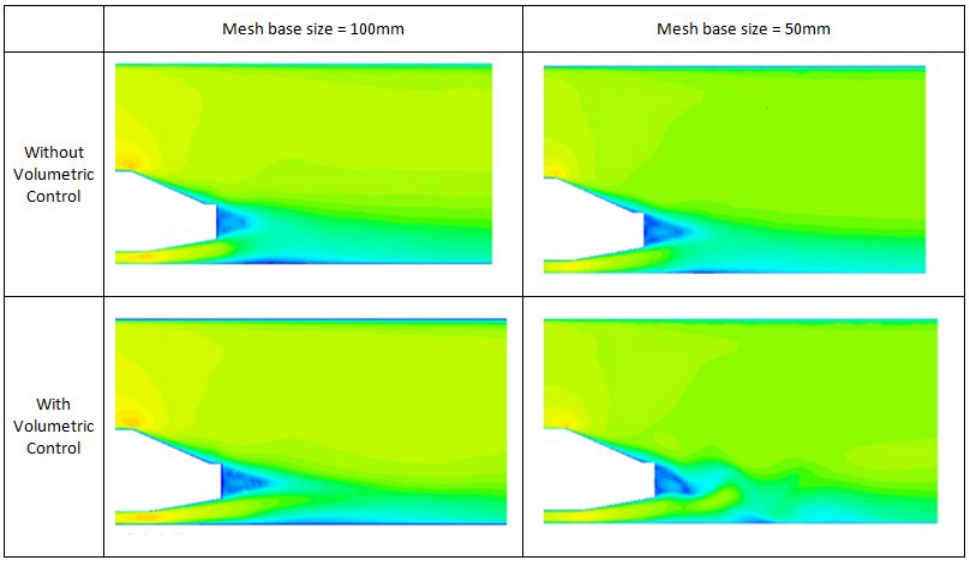

Figure 3. Velocity distribution for 100mm (left) and 50mm (right) mesh base size comparing without (top) and with (below) volumetric control.

From the results, it appears that the 50mm base mesh size with volumetric control provides a drag coefficient closest to the experimental data. However, if the result is compared with the same CFD model without volumetric control, the difference in drag coefficient is only 0.9%. However the simulation without volumetric control gave a significant reduction in simulation running time, providing a time saving of about 61%. Therefore, the 50mm mesh base size without volumetric control could be considered if computer speed or computation time is the determining factor.

4.2. Second Stage – Comparison between Full and Half Car Model

Further optimization of the CFD model selected above (50mm mesh base size without volumetric control) was carried out. The challenge here was to work in a memory limited environment, as optimizing the mesh required more computer memory. The computer memory needed is largely determined by the total number of cells. One way to reduce the cell count is by considering half a car with a symmetric boundary condition. This approach is technically valid only if both the car is geometrically symmetric about the centre line; therefore, if the car under body is asymmetric this approach may lead to erroneous results. It is also worth mentioning that this is only valid for steady flows where there is no significant lateral energy transfer across the symmetry plane in the wake.

Table 4 shows that using a half car model reduced the total number of cells by 43.62%. It also shows that the computation error in the drag coefficient between both models was less than 1%. As can be seen from figure 4 (below), the velocity distributions for both models are similar. These indicate that there is no significant difference between the full and half car models; and that the half car model can be used for further simulations. The main advantage of using a half car model is it gave a more than 50% reduction in the simulation run time.

TABLE 4: SIMULATION RESULTS COMPARING FULL CAR AND HALF CAR

	Full car	Half car	Percentage difference*
Total no of cells	409124	230682	43.62%
Drag Coefficient	0.3376	0.3404	0.84%
Simulation running time (min)	68.2	33.6	50.73%

* Percentage difference is calculated by adopting the full car as the reference.

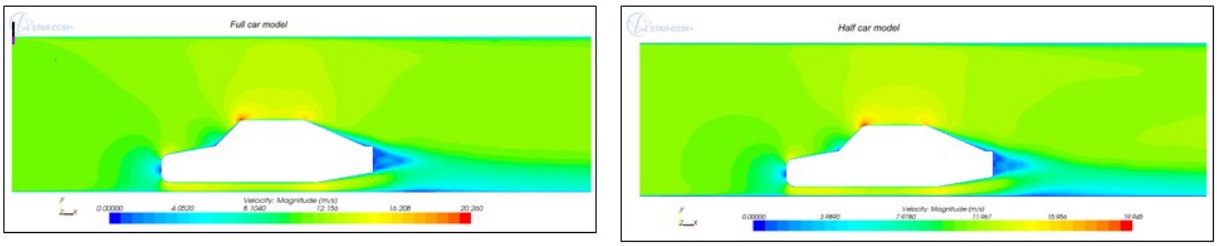

Figure 4. Velocity distribution for full (left) and half (right) car models

4.3. Third Stage – Mesh Parameter Optimization using Statistical Analysis

In stage 3, a statistical analysis technique was employed to examine which parameters have most influence on the final drag result. A half factorial experimental design was used to study the effects of the mesh parameters on drag coefficient, simulation run time and computer memory. Five mesh factors were selected in this study, each with two levels as listed in table 5 (below). The car surface mesh size represents the size of the cell attached to the car wall relative to the base size (50 mm). The surface growth rate represents how the cell size increases as it moves away from the wall. Prism layer thickness and number were also examined. Finally Polyhedral versus Trimmer mesh types were also investigated.

For a full factorial analysis 2^5= 32 runs would have to be considered. By using a half factorial design only 16 runs were required. The results were then analysed using the Minitab 15 statistical software package. A factorial analysis has to be carefully implemented in fluid flow analysis particularly when flow separation may occur. The numerical values of the parameter levels have to be chosen to be within the continuous trend and not having any discontinuity between the two selected level values.

TABLE 5: LIST OF MESH PARAMETERS (FACTORS) AND THEIR LEVELS

Factors	Level 1	Level 2
Car surface mesh size*	10%	15%
Surface growth rate	1.3	1.6
Mesh type	Polyhedral	Trimmer
No of prism layers	2	5
Prism layer thickness*	20%	33.3%

* Car surface mesh size and prism layer thickness are expressed as percentage of mesh base size.

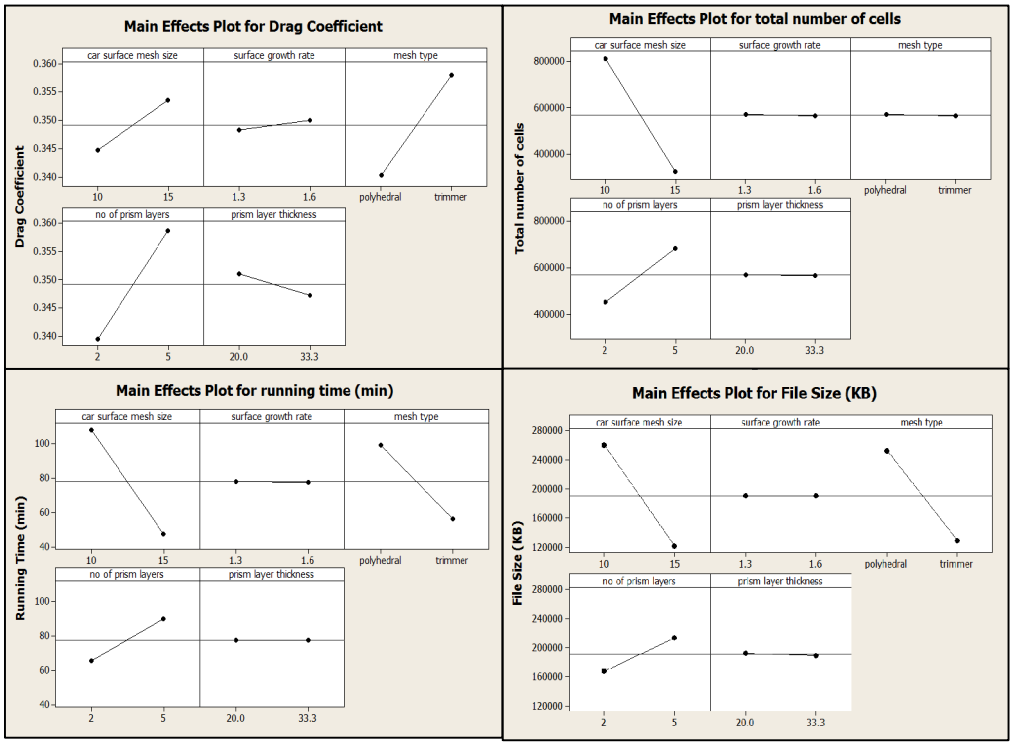

Figure 5. Main effects plot for each parameter on all responses

In the study, file size is used as a means of comparing the required computer memory as these two items are directly proportional to each other. Overall, the effects on simulation run time and file memory are analogous with total number of cells. It can be deduced that these two factors are very much dependent on cell counts.

As the car surface mesh size becomes smaller, the drag coefficient tends to reduce and approaches the experimental value, but this followed by an increase in the total number of cells as well as the simulation run time and the computer memory. Same pattern can be observed for surface growth rate but the effects of surface growth rate are not as major as car surface mesh size. From the effects of these two factors, it can be concluded that a more accurate result can be obtained by refining the surface mesh at the area of interest particularly at the rear of the car.

From the mesh optimization result, it shows that for almost the same number of cells, the polyhedral mesh structure gave more accurate results, but with a considerably higher amount of computing time and memory requirement compared to trimmer. For time-efficient computational logic, it is necessary to identify the grid nodal points. The conversion of differential equations into difference equations and further computing operations requires quick access to these points [15]. In trimmer, as all nodal points lie on grid lines they can be readily identified and accessed, whereas in a polyhedral mesh, the identification of the nodal points (polyhedral vertices) is not as straightforward. Thus, the access mechanisms to these points are more time consuming.

As can be seen from results in figure 6 (below), trimmer gave a less accurate prediction in the wake region for the same size of mesh. Polyhedral cells have the ability to permit a local increase in grid density as shown in figure 6. In order for trimmer to give the same accuracy as polyhedral, the grid density needs to be increased in the wake region.

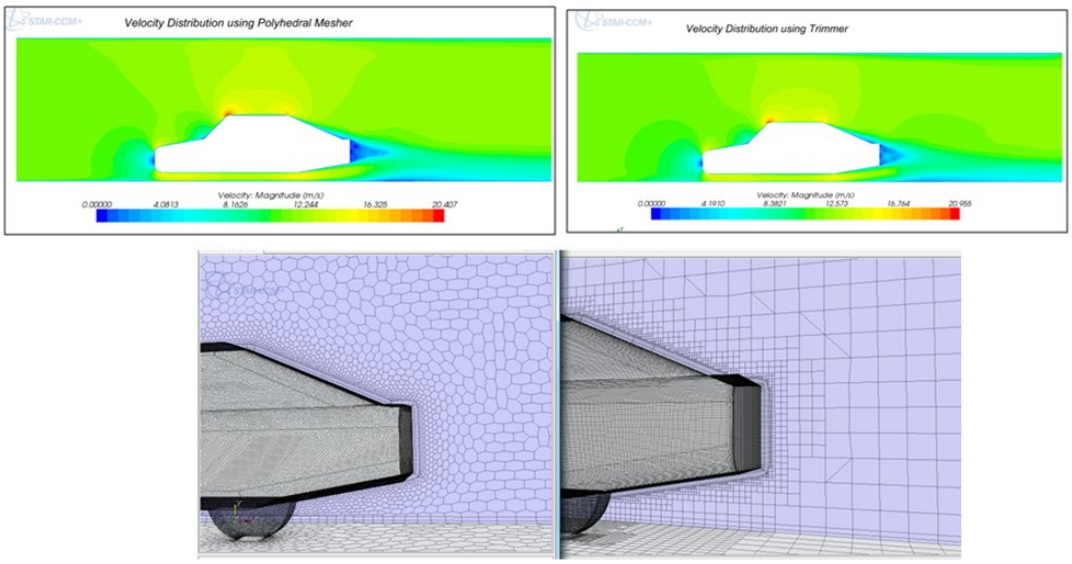

Figure 6. Comparison between polyhedral (left) and trimmer (right) meshing

While performing CFD simulations, if wall functions are to be applied, it is critical that the flow velocity within the boundary layer is captured within the logarithmic profile. The insertion of prism layers along the wall sections of the computational mesh surface is an effective way to treat the boundary layer. Results show that increasing the number of prism layers causes an increase in the total number of cells; while prism layer thickness does not affect cell count substantially. Prism layer parameters are chosen so that the law of the wall condition is valid and the best accuracy is obtained. The calculation of the wall Y+ value of the first interior node/grid helps to do that. As for this case, the combination of two prism layers with thickness 33.3% (16.65 mm) gave the value of drag coefficient closest to the MIRA data and the wall Y+ obtained was less than 160, which is below the maximum recommended limit [3].

According to statistical analysis using Minitab, the optimum mesh is achieved by the parameters values listed in Table 6:

TABLE 6: OPTIMIZED MESH OBTAINED FROM MINITAB ANALYSIS

Car surface mesh size	Surface growth rate	Mesh type	No of prism layers	Prism layer thickness	Drag coefficient	Percentage difference with MIRA C_D	Total no of cells	Running time (min)	File size (KB)
10%	1.3	polyhedral	2	33.3%	0.3215	0.23%	622460	112.48	293158

The optimized mesh gave a drag coefficient 0.23% higher than the MIRA experimental value. Reducing the car surface growth rate from 1.3 to 1.25 will match the experimental value but at the cost of a significant increase in running time, 36% as shown in table 7.

TABLE 7: FURTHER MESH REFINEMENT BY REDUCING SURFACE GROWTH RATE

Car surface mesh size	Surface growth rate	Drag coefficient, C_D	Percentage difference with MIRA C_D	Total no of cells	Running time (min)	File Size (KB)
10%	1.25	0.3208	0.018%	648962	153.46	306765

4.4. 4th Stage – Changes in Mesh Parameters as the Car Size Becomes Smaller

Following the results obtained for the 1:3 scale model, the optimized CFD model was implemented on 1:4 and 1:5 scale models. The results are shown in table 8 below:

TABLE 8: DRAG COEFFICIENTS RESULTS FOR 1:4 AND 1:5 SCALE MODELS

Model scale	MIRA C_D data	CFD C_D data	Percentage difference*
1:4	0.2706	0.2947	8.91%
1:5	0.2653	0.2894	9.10%

* Percentage difference is calculated by adopting MIRA data (C_D = 0.2706 for 1:4 and C_D = 0.2653 for 1:5) as the reference.

According to table 8, the drag coefficients obtained were much higher than the MIRA data. Based on the mesh optimization study made on the 1:3 model, a better prediction of drag coefficient can be obtained by further refining the mesh base size, mesh on car the surface and optimizing the prism layer parameters.

The mesh base size was decreased in proportion to the car length. This assumption is based on considering the flow pattern around the vehicle is changing as the cars were scaled down, therefore the mesh has to be reduced accordingly. Keeping in mind that Reynolds number was kept constant at 10^6 for the three car sizes during the wind tunnel test. The proportionality of cell size to car length will lead to similar inertia to viscous forces for each cell in the flow domain. Reducing all the mesh sizes by scaling them to the car size can be done be changing only the base size in STAR-CCM+. The car surface mesh and prism layer thickness are reduced accordingly as they are expressed as percentage of mesh base. The calculated drag coefficients for the other two scaled models 1:4 and 1:5 in comparison to the wind tunnel measured values are listed in table 9.

TABLE 9: DRAG COEFFICIENTS FOR 1:4 AND 1:5 SCALE MODELS BY SCALING DOWN THE MESH BASE SIZE IN PROPORTION TO CAR LENGTH

Model scale	Mesh base size = 3.6% x car length	Drag coefficient, C_D	Percentage difference with MIRA C_D
1:4	37.5mm	0.2849	5.31%
1:5	30mm	0.2717	2.43%

Comparing the calculated drag value presented in Table 8 with that in Table 9, it is clear that reducing the mesh relative to the car length leads to a more accurate prediction for the drag coefficient. It also shows that the mesh sizes must be adjusted in proportion to the car length. Applying this method keeps wall Y+ for both models within the acceptable range (less than 160).

Further refinement can be continued to reduce the difference between the predicted drag coefficient and the measured value. The most effective parameter is the surface mesh size. Figure 7 shows the effect of reducing the surface mesh size on the predicted drag coefficient.

Figure 7. Effect of car surface mesh size on drag coefficient

It is obvious that as the car surface mesh becomes smaller, the drag coefficient reduces and approaches the measured value (MIRA data). By looking at the trends shown in the graph, it can be said that both models have almost reached their optimum size of car surface mesh, as the difference in drag coefficient between the two mesh sizes is small and further refining the mesh will not have any significant effect on the drag coefficient result. This is obvious for the 1:4 scale model. Even though for the 1:5 scale model the drag coefficient value increased for the last point, the difference between the last two mesh sizes is small, about 0.2%. So, it can be assumed that the optimum car surface mesh size for the 1:4 scale model is 0.21% of the car length and 0.177% of the car length for the 1:5 scale model.

Figure 8 (below) shows the relationship between car length and its optimum car surface mesh size. The percentage of the optimum car surface mesh size to car length decreases as the car size reduces. It also shows that as the model size decreases, the optimum percentage of the car surface mesh size to car length might reach a minimum value. A further study can be done by having few more model sizes to confirm on this relationship; also, the car surface mesh size for the 1:3 scale model should be refined until it reaches its optimum value, even though the drag coefficient result will differ from the MIRA data.

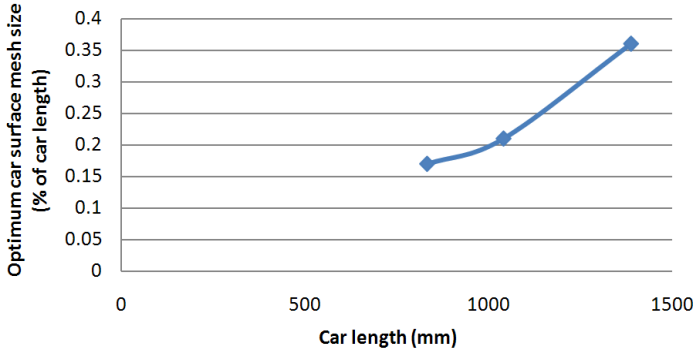

Figure 8. Optimum car surface mesh size by car length

To sum up the actions taken for optimizing the mesh, the same mesh parameters cannot be used if the model sizes are different. As a rough guideline, the mesh size for the wind tunnel needs to be adjusted in proportion to the car length; this means that a smaller car model will need a finer mesh. In this case, the proportion of the mesh size to the car length is 3.6%. For this case, two prism layers with overall thickness of 33.3% of the base mesh size

gave a good approximation of the boundary layer for all the scale models. The optimum car surface mesh size also needs to be refined in proportion to the car length.

4.5. The Final Results of CFD Models

By reducing the car surface mesh size and mesh base size, it was possible to produce a more accurate drag coefficient that is closer to the wind tunnel measured value. The final value of the drag coefficient for the three car model sizes and their corresponding mesh base size and car surface sizes are presented in Table 10 below.

TABLE 10: DRAG COEFFICIENTS FROM MIRA EXPERIMENT AND CFD SIMULATIONS

Scale model	Car length (mm)	Mesh base size = 3.6% x car length (mm)	Car surface mesh size (% car length)	MIRA C_D data	CFD C_D data	Percentage difference*
1:3	1388	50	0.36%	0.3208	0.3215	0.23%
1:4	1041	37.5	0.21%	0.2706	0.2812	3.91%
1:5	833	30	0.18%	0.2653	0.2675	0.83%

* Percentage difference is calculated by adopting MIRA data as the reference.

It can be concluded that the CFD simulations of the drag coefficient are in reasonable agreement with the MIRA data, as the maximum difference is only 3.91%. The differences can be due to many factors; for instance, the difference in drag coefficients measured by different wind tunnels on the same car can be up to 5% [14]. Realistically, there are also errors in the CFD simulations due to a variety of factors [14].

5. Conclusion

This study shows that with mesh optimization it is possible using a PC to make accurate predictions of the drag coefficient within 4% of the wind tunnel measured value. The major parameters used to generate the mesh in STAR-CCM+ that can significantly affect the drag value with minimum use of memory and time for the fast-back car model used in this study can be summarized in the following points:

- Polyhedral mesh provides better resolution than the trimmer type of mesh of the flow in the wake region with fewer cells, however more computational time and memory is needed.
- Having regions of different mesh sizes (volumetric control) around the vehicle could consume more memory and time than having a mesh with constant growth rate.
- Reducing the size of the mesh attached to the car surface and its growth rate has a significant effect on the solution and they are considered the most important parameters, nevertheless y+ has to within the valid range.
- The optimized mesh setting value for the 1:3 scale fast-back car model has been identified and for different car sizes the base mesh setting has to be scaled to the length of the car.
- Further reduction in the mesh attached to the car surface may be required if the model size becomes smaller to achieve better accuracy.

References

[1] Yang, Z., Schenkel, M., Assessment of Closed-Wall Wind Tunnel Blockage Using CFD. SAE Technical Paper 2004-01-0672, 2004.

[2] Murad, N., Naser, J., Alam, F., Watkins, S., Simulation of Vehicle A-Pillar Aerodynamics using Various Turbulence Models. SAE Technical Paper 2004-01-0231, 2004.

[3] Connor, C., Kharazi, A., Walter, J., Martindale, B., Comparison of Wind Tunnel Configurations for Testing Closed-Wheel Race Cars: A CFD Study. SAE Technical Paper 2006-01-3620, 2006.

[4] Soni, B.K., Koomullil, R., Thompson, D.S., Thornburg, H., Solution Adaptive Grid Strategies Based on Point Redistribution. Comput. Methods Appl. Mech. Engrg., 2000. Vol. 189, pp 1183-1204.

[5] Jin, C., Xu, K., An Adaptive Grid Method for Two-Dimensional Viscous Flows. Journal of Computational Physics, 2006. Vol. 218, pp 68-81.

[6] Society of Automotive Engineers, Closed-Test-Section Wind Tunnel Blockage Corrections for Road Vehicles. SAE SP-1176 Warrendale: Society of Automotive Engineers, Inc. 1996.

[7] Mokhtar, W.A, Britcher, C.P., Boundary Interference of High Blockage Models in Open Jet Test Sections. SAE Technical Paper 2008-01-1201, 2008.

[8] Gleason, M. E., Detailed Analysis of the Bluff Body Blockage Phenomenon in Closed Wall Wind Tunnels Utilizing CFD. SAE Technical Paper 2007-01-1046, 2007.

[9] Brown, M A, Baxendale, A J and Hickman, D Recent Enhancements of the MIRA Model Wind-Tunnel, 2nd MIRA International Conference on Vehicle Aerodynamics, 20-21 October 1998, Hilton National Hotel, Coventry.

[10] Singh, R., Automated Aerodynamic Design Optimization Process for Automotive Vehicle. SAE Technical Paper 2003-01-0993, 2003.

[11] Axelsson N., Ramnefors M., Gustafson R., Accuracy in Computational Aerodynamics Part 1: Stagnation Pressure. SAE Technical Paper 980037, 1998.

[12] Yang, Z., Nastov, A., Schenkel, M., Further Assessment of Closed-Wall Wind Tunnel Blockage Using CFD. SAE Technical Paper 2005-01-0868, 2005.

[13] Moky, M., Wall Interference correction to drag measurements in Automotive Wind Tunnels. Journal of Wind Engineering and Industrial Aerodynamics, 1995. Vol. 56, Issues2-3, pp107-12.

[14] Hucho,W.,(ed) 4th edition Aerodynamics of Road Vehicles. Warrendale: Society of Automotive Engineers, Inc. 1998.

[15] Stern, F., Wilson, R. and Shao, J. Quantitative V&V of CFD Simulations and Certifications of CFD Codes. International Journal of Numerical Methods in Fluids, 2006. Vol. 50, Issue 11, pp 1335-1355.